

Evolution of Threading Dislocation Density and Stress in GaN Films Grown on (111) Si Substrates by Metalorganic Chemical Vapor Deposition

X. WENG,¹ J.D. ACORD,¹ A. JAIN,¹ E.C. DICKEY,¹ and J.M. REDWING^{1,2}

1.—Department of Materials Science and Engineering and Materials Research Institute, The Pennsylvania State University, University Park, PA, 16802, USA. 2.—E-mail: jmr31@psu.edu

We have studied the evolution of threading dislocations (TDs), stress, and cracking of GaN films grown on (111) Si substrates using a variety of buffer layers including thin AlN, compositionally graded $\text{Al}_x\text{Ga}_{1-x}\text{N}$ ($0 \leq x \leq 1$), and AlN/ $\text{Al}_y\text{Ga}_{1-y}\text{N}$ / $\text{Al}_x\text{Ga}_{1-x}\text{N}$ ($0 \leq x \leq 1$, $y = 0$ and 0.25) multilayer buffers. We find a reduction in TD density in GaN films grown on graded $\text{Al}_x\text{Ga}_{1-x}\text{N}$ buffer layers, in comparison with those grown directly on a thin AlN buffer layer. Threading dislocation bending and annihilation occurs in the region in the graded $\text{Al}_x\text{Ga}_{1-x}\text{N}$ grown under a compressive stress, which leads to a decrease of TD density in the overgrown GaN films. In addition, growing a thin AlN/ $\text{Al}_y\text{Ga}_{1-y}\text{N}$ bilayer prior to growing the compositionally graded $\text{Al}_x\text{Ga}_{1-x}\text{N}$ buffer layer significantly reduces the initial TD density in the $\text{Al}_x\text{Ga}_{1-x}\text{N}$ buffer layer, which subsequently further reduces the TD density in the overgrown GaN film. In-situ stress measurements reveal a delayed compressive-to-tensile stress transition for GaN films grown on graded $\text{Al}_x\text{Ga}_{1-x}\text{N}$ buffer layers or multilayer buffers, in comparison to the film grown on a thin AlN buffer layer, which subsequently reduces the crack densities in the films.

Key words: GaN, Si substrates, buffer layers, dislocations, stress

INTRODUCTION

GaN films are generally grown on sapphire, SiC, or (111) Si substrates. Compared to sapphire and SiC, (111) Si substrates have several advantages including high quality, low cost, large wafer size, and the potential integration of high-speed and high-power nitride devices with Si microelectronics. A thin AlN buffer layer is often used for the growth of GaN films on Si substrates.¹ Due to the large lattice mismatch between Group III-nitrides and Si, a high density of threading dislocations (TDs) will form in the heteroepitaxial nitride films.² Furthermore, thick (>250 nm) GaN films grown on Si using thin (~ 100 nm) AlN buffer layers often crack during the postgrowth cooling process due to the tensile coefficient of thermal expansion (CTE) mismatch stress and the additional tensile growth

stress arising from island coalescence and lateral grain growth.³ In order to use Si as a substrate for GaN films, it is necessary to reduce the TD density while simultaneously inhibiting the film cracking.

Compositionally graded $\text{Al}_x\text{Ga}_{1-x}\text{N}$ buffer layers have been used to reduce crack density in GaN films grown on (111) Si in several studies.^{4–7} In-situ stress measurements suggest that the composition-graded induced compressive lattice mismatch stress in the $\text{Al}_x\text{Ga}_{1-x}\text{N}$ buffer layers compensates the tensile CTE mismatch stress and growth stress, thus alleviating the cracking of the GaN films.^{6–8} On the other hand, limited studies have been carried out on the effects of the $\text{Al}_x\text{Ga}_{1-x}\text{N}$ buffer layers on the TD evolution in GaN films grown on (111) Si substrates.^{4,5,7} Our recent study showed a decrease in TD density from $(1.5 \pm 0.3) \times 10^{10}$ to $(1.1 \pm 0.2) \times 10^{10} \text{ cm}^{-2}$ for $\sim 1\text{-}\mu\text{m}$ -thick GaN films grown on a thin AlN buffer layer and a $1\text{-}\mu\text{m}$ composition graded $\text{Al}_x\text{Ga}_{1-x}\text{N}$ ($0 \leq x \leq 1$) buffer layer, respectively.⁹ Furthermore, by using an AlN/GaN/ $\text{Al}_x\text{Ga}_{1-x}\text{N}$ multilayer buffer instead of a single

(Received August 24, 2006; accepted October 27, 2006; published online January 31, 2007)

graded $\text{Al}_x\text{Ga}_{1-x}\text{N}$ buffer layer, the TD density of the overgrown GaN film was further reduced to $(6.1 \pm 1.4) \times 10^9 \text{ cm}^{-2}$.⁹ Thus, the $\text{AlN}/\text{GaN}/\text{Al}_x\text{Ga}_{1-x}\text{N}$ multilayer buffer is promising for the growth of low TD density GaN films on (111) Si substrates. However, the effects of such multilayer buffers on the evolution of stress and cracking of the GaN films are not known. In this article, we report our comprehensive investigation of the evolution of TDs, stress, and cracking of GaN films grown on (111) Si substrates using a variety of buffer layers. These buffer layers include a single compositionally graded $\text{Al}_x\text{Ga}_{1-x}\text{N}$ ($0 \leq x \leq 1$) buffer layer and two $\text{AlN}/\text{Al}_y\text{Ga}_{1-y}\text{N}/\text{Al}_x\text{Ga}_{1-x}\text{N}$ multilayer buffers with $y = 0$ and 0.25. A GaN film grown on a thin (100 nm) AlN buffer layer is also studied for comparison.

EXPERIMENTAL PROCEDURES

All the layers were grown by metalorganic chemical vapor deposition in a vertical reactor at 1,100°C and 50 Torr on 500- μm -thick $1 \times 1 \text{ cm}$ (111) Si substrates. Purified hydrogen was used as the carrier gas at 8 standard liter per minute (slpm). The precursor flow rates were 4 slpm, ~ 0.5 standard cubic centimeter per minute (sccm), and ~ 0.2 sccm for ammonia, trimethyl aluminum (TMA), and trimethyl gallium (TMG), respectively. The composition grading of the $\text{Al}_x\text{Ga}_{1-x}\text{N}$ ($0 \leq x \leq 1$) layer was achieved by simultaneously ramping down/up the TMA/TMG gas flow rates during growth. The growth rate of the layers was 1–2 $\mu\text{m}/\text{h}$. The nominal thicknesses of the GaN films investigated in this study were all 500 nm. The thickness of the compositionally graded $\text{Al}_x\text{Ga}_{1-x}\text{N}$ buffer layer was 1 μm , while the thicknesses of the AlN and the $\text{Al}_y\text{Ga}_{1-y}\text{N}$ layers of the $\text{AlN}/\text{Al}_y\text{Ga}_{1-y}\text{N}/\text{Al}_x\text{Ga}_{1-x}\text{N}$ multilayer buffers were both 80 nm. The substrate curvature change during growth resulting from stress in the film was measured in-situ using a multibeam optical stress sensor (MOSS) system. The curvature change was related to film stress using the Stoney equation.¹⁰ For transmission electron microscopy (TEM)

studies, both cross-sectional and plan-view TEM specimens were prepared using conventional mechanical thinning followed by argon ion milling. The TEM imaging was carried out on JEOL (Japan Electron Optics Ltd., Tokyo) 2010F and 2010 LaB₆ microscopes operated at 200 keV. To determine the TD density, 10 plan-view images were collected from different regions with a total area of $\sim 20 \mu\text{m}^2$ for each GaN film. Because the TDs are a -type edge dislocations or $(a + c)$ -type mixed dislocations,^{7,9} all the plan-view images were collected under multibeam diffraction conditions near the GaN [0001] zone axis to reveal all TDs. For the cross-sectional TEM study, bright-field imaging using multibeam diffraction conditions near the GaN [1 $\bar{1}$ 00] zone axis was used, which also revealed all types of TDs. Nomarski optical microscopy was employed to examine the cracking of the GaN films grown on various buffer layers.

RESULTS AND DISCUSSION

Evolution of TDs

Figure 1 shows typical plan-view TEM images of the 500-nm GaN films grown on (a) a 100-nm AlN buffer layer and (b) a 1- μm compositionally graded $\text{Al}_x\text{Ga}_{1-x}\text{N}$ buffer layer. The TD densities for the films grown on AlN and $\text{Al}_x\text{Ga}_{1-x}\text{N}$ are $(4.6 \pm 0.3) \times 10^{10}$ and $(1.6 \pm 0.1) \times 10^{10} \text{ cm}^{-2}$, respectively. Thus, the TD density is reduced by using a graded $\text{Al}_x\text{Ga}_{1-x}\text{N}$ instead of a thin AlN buffer layer, similar to the results of our earlier study.⁹

The TD evolution in the growth direction of these two samples is revealed by cross-sectional TEM images. As shown in Fig. 2a, the thin AlN buffer layer grown on the Si substrate is highly defective, where individual TDs cannot be discriminated due to the TD overlapping. This high density of TDs results from the 19% lattice mismatch between AlN and Si. The strain contrast within the Si substrate near the AlN/Si interface is also a result of this 19% lattice mismatch. The initial TD density in the GaN film near the AlN/GaN interface appears much

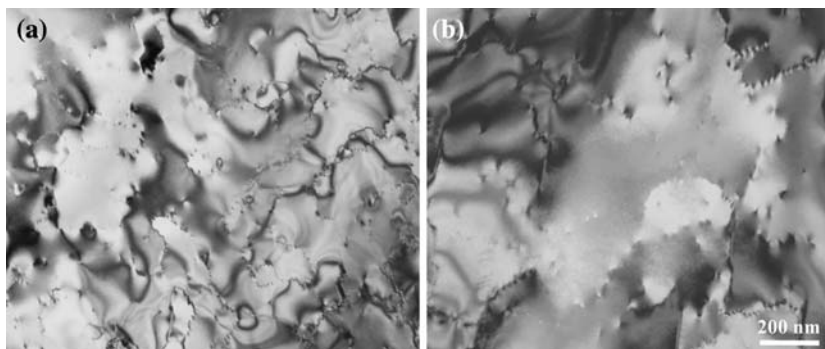


Fig. 1. Typical plan-view TEM images of the GaN films grown on (a) a thin AlN buffer layer and (b) a graded $\text{Al}_x\text{Ga}_{1-x}\text{N}$ buffer layer. Both images were collected under multibeam diffraction contrast conditions near the GaN [0001] zone axis to reveal all TDs.

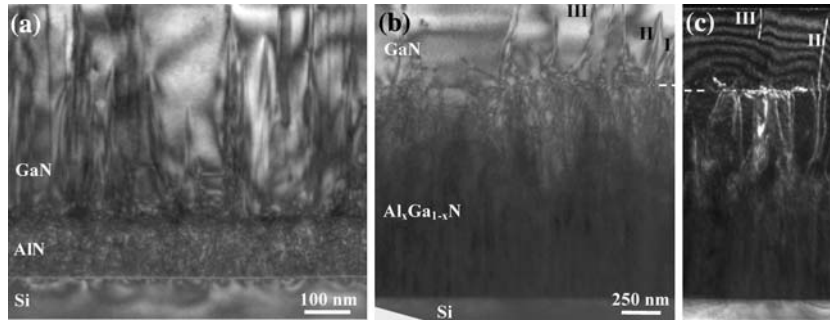


Fig. 2. Cross-sectional TEM images of the GaN films grown on (a) a thin AlN buffer layer and (b) a graded $\text{Al}_x\text{Ga}_{1-x}\text{N}$ buffer layer. Both images were collected under multibeam diffraction contrast conditions near the $[1\bar{1}00]$ zone axis to reveal all TDs. A $[0002]$ weak beam dark-field image corresponding to the right half of (b) is shown in (c), which reveals TDs with a screw component. The dashed line in (b) and (c) indicates the position of the film/buffer interface.

lower than that in the AlN, suggesting that most of the TDs in the AlN layer end at the AlN/GaN interface without threading into the overgrown GaN film. In addition to some TDs continuing from the AlN buffer layer, the TDs in the GaN film near the AlN/GaN interface may arise from the 2.5% lattice mismatch between AlN and GaN. The TD bending and annihilation is apparent in the first ~ 80 nm of the GaN film, which leads to a quick reduction in TD density. Nonetheless, the TD lines in the remaining part of the GaN film are nearly parallel to the growth direction and little bending and annihilation is observed, such that a relatively high TD density persists in the film.

For the $\text{GaN}/\text{Al}_x\text{Ga}_{1-x}\text{N}/\text{Si}$ ($0 \leq x \leq 1$) heterostructure, the lattice mismatch between $\text{Al}_x\text{Ga}_{1-x}\text{N}$ and Si ($x = 1$ at the interface) is also 19%. Therefore, similar to the thin AlN buffer layer shown in Fig. 2a, a very high initial TD density in the $\text{Al}_x\text{Ga}_{1-x}\text{N}$ layer near the $\text{Al}_x\text{Ga}_{1-x}\text{N}/\text{Si}$ interface is also observed. As shown in Fig. 2b, a dark contrast is also evident in the graded $\text{Al}_x\text{Ga}_{1-x}\text{N}$ buffer layer near the buffer/Si interface, where individual TDs cannot be distinguished. It is also evident in Fig. 2b, and the corresponding $[0002]$ weak beam dark-field image

shown in Fig. 2c, that significant bending of TDs occurs in the top half of the graded $\text{Al}_x\text{Ga}_{1-x}\text{N}$ buffer layer, similar to our earlier observations.^{7,9} Because the majority of the TDs are a -type edge dislocations,^{7,9} only a few $(a + c)$ -type TDs in the GaN film are revealed in Fig. 2c.

The TD bending prevents the TDs from threading through the buffer layer and entering the GaN film and also enhances the TD interaction and annihilation. As a result, despite the very high initial TD density in the $\text{Al}_x\text{Ga}_{1-x}\text{N}$ layer, the initial TD density in the overgrown GaN film near the GaN/ $\text{Al}_x\text{Ga}_{1-x}\text{N}$ interface appears lower than that in the GaN film near the GaN/AlN interface shown in Fig. 2a. In addition, Fig. 2b also shows TD bending within the GaN film, which further reduces the TD density of the GaN film. Thus, the TD density of the GaN film grown on the compositionally graded $\text{Al}_x\text{Ga}_{1-x}\text{N}$ buffer is significantly lower than that of the film grown on the thin AlN buffer layer.

In order to further reduce the TD density in the GaN film, we replace the single compositionally graded $\text{Al}_x\text{Ga}_{1-x}\text{N}$ buffer layer with $\text{AlN}/\text{Al}_y\text{Ga}_{1-y}\text{N}/\text{Al}_x\text{Ga}_{1-x}\text{N}$ multilayer buffers. As shown in Fig. 3, instead of growing the graded $\text{Al}_x\text{Ga}_{1-x}\text{N}$ buffer layer

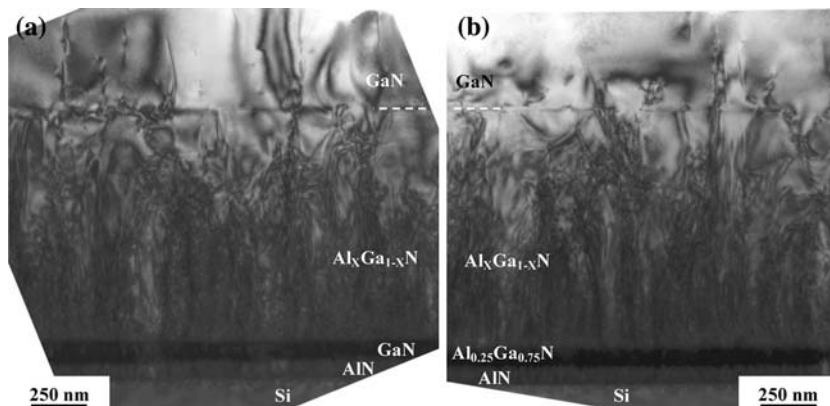


Fig. 3. Cross-sectional TEM images of the GaN films grown on (a) the $\text{AlN}/\text{GaN}/\text{Al}_x\text{Ga}_{1-x}\text{N}$ and (b) the $\text{AlN}/\text{Al}_{0.25}\text{Ga}_{0.75}\text{N}/\text{Al}_x\text{Ga}_{1-x}\text{N}$ multilayer buffers. Both images were collected under multibeam diffraction contrast conditions near the $[1\bar{1}00]$ zone axis to reveal all TDs. The dashed line in each image indicates the position of the film/buffer interface.

directly on the Si substrate with a 19% lattice mismatch, we grow the graded $\text{Al}_x\text{Ga}_{1-x}\text{N}$ buffer layer on a thin $\text{AlN}/\text{Al}_y\text{Ga}_{1-y}\text{N}$ bilayer with (a) $y = 0$ or (b) 0.25. As a result, the lattice mismatch between the graded $\text{Al}_x\text{Ga}_{1-x}\text{N}$ buffer layer and the layer below is reduced to less than -2.5% , which subsequently leads to a significant reduction in the initial TD density in the graded $\text{Al}_x\text{Ga}_{1-x}\text{N}$ buffer layer.

The decrease of the initial TD densities in the graded $\text{Al}_x\text{Ga}_{1-x}\text{N}$ buffer layers grown on the thin $\text{AlN}/\text{Al}_y\text{Ga}_{1-y}\text{N}$ bilayers is illustrated in Fig. 4a and b, which are higher magnification images collected near the Si substrates of the two samples shown in Fig. 3. In both Fig. 4a and b, a very high TD density is evident in the thin AlN layer due to the 19% lattice mismatch between AlN and Si. In contrast, individual TDs can be discriminated in the graded $\text{Al}_x\text{Ga}_{1-x}\text{N}$ buffer layers grown on the thin GaN and $\text{Al}_{0.25}\text{Ga}_{0.75}\text{N}$ layers, suggesting a significantly lower TD density in the $\text{Al}_x\text{Ga}_{1-x}\text{N}$ layers than in the AlN layers. As discussed earlier, the initial TD density in an $\text{Al}_x\text{Ga}_{1-x}\text{N}$ layer grown directly on a Si substrate is expected to be similar to that in an AlN layer grown on Si due to the same 19% lattice mismatch. Therefore, the initial TD density can be reduced by growing the graded $\text{Al}_x\text{Ga}_{1-x}\text{N}$ buffer layer on the thin $\text{AlN}/\text{Al}_y\text{Ga}_{1-y}\text{N}$ bilayers instead of growing directly on Si substrates.

The insertion of the thin $\text{AlN}/\text{Al}_y\text{Ga}_{1-y}\text{N}$ bilayers does not affect the bending of TDs in the graded $\text{Al}_x\text{Ga}_{1-x}\text{N}$ buffer layers. As shown in Fig. 3, significant bending and annihilation occurs in the top half of the $\text{Al}_x\text{Ga}_{1-x}\text{N}$ buffer layers, similar to the $\text{Al}_x\text{Ga}_{1-x}\text{N}$ buffer layer on Si shown in Fig. 2b and c. Such bending and annihilation, combined with the reduced initial TD density, leads to a further reduced TD density in the GaN films grown on the $\text{AlN}/\text{Al}_y\text{Ga}_{1-y}\text{N}/\text{Al}_x\text{Ga}_{1-x}\text{N}$ multilayer buffers compared to that grown on a single graded $\text{Al}_x\text{Ga}_{1-x}\text{N}$ buffer layer. Figure 5 shows two typical plan-view TEM images of the GaN films grown on (a) the $\text{AlN}/\text{GaN}/\text{Al}_x\text{Ga}_{1-x}\text{N}$ and (b) the $\text{AlN}/\text{Al}_{0.25}\text{Ga}_{0.75}\text{N}/\text{Al}_x\text{Ga}_{1-x}\text{N}$ multilayer buffers. The TD densities of these two GaN films are $(1.3 \pm 0.1) \times 10^{10}$ and $(8.4 \pm 1.6) \times 10^9 \text{ cm}^{-2}$, respectively, which are both lower than that of the GaN film grown on a single graded $\text{Al}_x\text{Ga}_{1-x}\text{N}$ buffer layer.

It is interesting to note that the TD density of the GaN film grown on the $\text{AlN}/\text{Al}_{0.25}\text{Ga}_{0.75}\text{N}/\text{Al}_x\text{Ga}_{1-x}\text{N}$ multilayer buffer is lower than that of the film grown on the $\text{AlN}/\text{GaN}/\text{Al}_x\text{Ga}_{1-x}\text{N}$ multilayer buffer. This is likely due to the lower lattice mismatch between $\text{Al}_{0.25}\text{Ga}_{0.75}\text{N}$ and $\text{Al}_x\text{Ga}_{1-x}\text{N}$ than between GaN and $\text{Al}_x\text{Ga}_{1-x}\text{N}$ ($x = 1$ at the interface), and the subsequent lower initial TD density in the $\text{Al}_x\text{Ga}_{1-x}\text{N}$ buffer layer on the thin $\text{AlN}/\text{Al}_{0.25}\text{Ga}_{0.75}\text{N}$ bilayer.

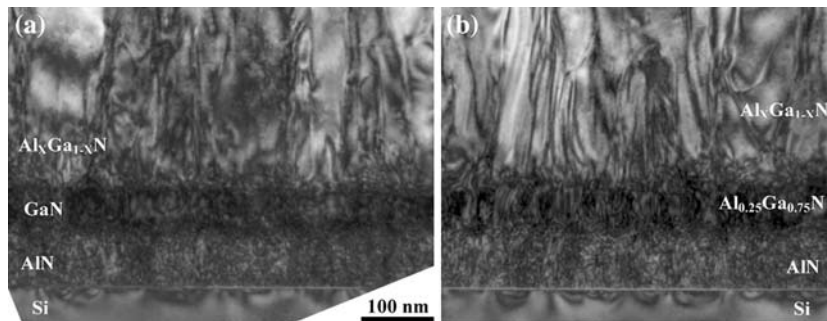


Fig. 4. Higher magnification cross-sectional TEM images of the GaN films grown on (a) the $\text{AlN}/\text{GaN}/\text{Al}_x\text{Ga}_{1-x}\text{N}$ and (b) the $\text{AlN}/\text{Al}_{0.25}\text{Ga}_{0.75}\text{N}/\text{Al}_x\text{Ga}_{1-x}\text{N}$ multilayer buffers. Both images were collected near the Si substrates under multibeam diffraction contrast conditions near the [1100] zone axis to reveal all TDs.

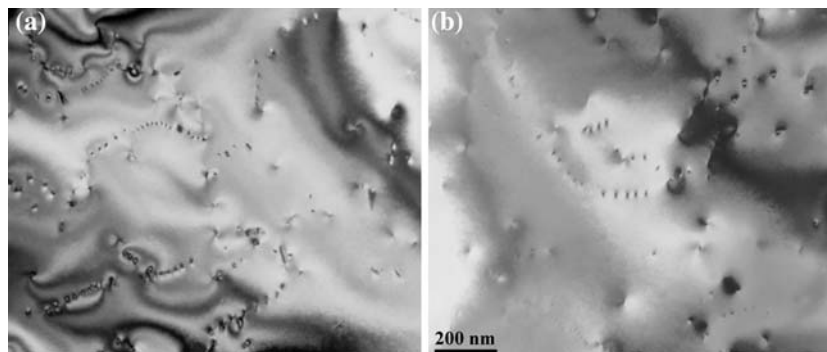


Fig. 5. Plan-view TEM images of the GaN films grown on (a) the $\text{AlN}/\text{GaN}/\text{Al}_x\text{Ga}_{1-x}\text{N}$ and (b) the $\text{AlN}/\text{Al}_{0.25}\text{Ga}_{0.75}\text{N}/\text{Al}_x\text{Ga}_{1-x}\text{N}$ multilayer buffers. Both images were collected near the [0001] zone axis to reveal all TDs.

Thus, increasing the Al content in the $\text{Al}_y\text{Ga}_{1-y}\text{N}$ layer may further decrease the initial TD density in the graded $\text{Al}_x\text{Ga}_{1-x}\text{N}$ buffer layer and the TD density in the overgrown GaN film. Further studies are currently in progress.

Stress Evolution and Film Cracking

Substrate curvature was monitored during the growth using the MOSS system, and the stress-thickness product versus layer thickness plot was obtained for each sample. Figure 6a shows a representative plot, which is from the GaN/ $\text{Al}_x\text{Ga}_{1-x}\text{N}$ / $\text{Al}_{0.25}\text{Ga}_{0.75}\text{N}$ /AlN/Si heterostructure. A positive slope of the curve indicates a tensile growth stress, while a negative slope indicates a compressive growth stress. Small peaks, such as those denoted by “P” in Fig. 6a, are often observed in the plots. These are artifacts related to the intensity extinction of the laser spots caused by the interference between the laser beams reflected from the epilayer surface and those reflected from the Si surface during the data collection.

The thin AlN layer of the AlN/ $\text{Al}_{0.25}\text{Ga}_{0.75}\text{N}$ / $\text{Al}_x\text{Ga}_{1-x}\text{N}$ multilayer buffer grows under a tensile stress, as shown in Fig. 6a. Similarly, the thin AlN layer of the AlN/GaN/ $\text{Al}_x\text{Ga}_{1-x}\text{N}$ multilayer buffer and the AlN buffer of the GaN/AlN/Si heterostructure also grow under a tensile stress. This tensile stress has been attributed to the combination of lattice mismatch stress and AlN island coalescence induced stress.¹¹ The thin GaN and $\text{Al}_{0.25}\text{Ga}_{0.75}\text{N}$ layers of the multilayer buffers both grow under a compressive stress as a result of their larger lattice parameter compared to AlN. The growth stress of each compositionally graded $\text{Al}_x\text{Ga}_{1-x}\text{N}$ buffer layer is initially tensile and gradually transitions to compressive. The initial tensile stress in the single $\text{Al}_x\text{Ga}_{1-x}\text{N}$ buffer layer grown directly on the Si substrate has been attributed to island coalescence and lateral grain growth.⁶ For the $\text{Al}_x\text{Ga}_{1-x}\text{N}$ layer of the multilayer buffers, the lattice mismatch between $\text{Al}_x\text{Ga}_{1-x}\text{N}$ and $\text{Al}_y\text{Ga}_{1-y}\text{N}$ also contributes to the tensile stress. As the growth continues, the

composition grading-induced compressive stress offsets the tensile stress, which gradually leads to the tensile-to-compressive stress transition near the half-thickness of the $\text{Al}_x\text{Ga}_{1-x}\text{N}$ layer.⁶ A comparison between the stress curves and cross-sectional TEM images such as those shown in Figs. 6a and 3b suggests that the TD bending and annihilation in the $\text{Al}_x\text{Ga}_{1-x}\text{N}$ layer mainly occurs when the layer is under compressive growth stress. This is consistent with observations reported in several recent studies.^{7,8,12}

The evolution of growth stress in the GaN films grown on different buffer layers is shown in Fig. 6b. For the GaN film grown on a thin AlN buffer layer, the stress is initially compressive but transitions to tensile after a thickness of ~ 80 nm. As described earlier, the cross-sectional TEM image shown in Fig. 2a indicates that TD bending and annihilation is apparent only in the first ~ 80 nm of this GaN film. This further suggests that the TD bending occurs only when the film is under compressive stress. The GaN films grown on the single graded $\text{Al}_x\text{Ga}_{1-x}\text{N}$ buffer layer and the multilayer buffers also start to grow under compressive stress, which gradually relaxes as the films grow. This relaxation of the compressive stress may be due to the TD bending. The bending of the a -type edge TDs and $(a+c)$ -type mixed TDs leads to the formation of misfit dislocation segments, which contributes to the relaxation of compressive stress.^{12–14} It has been predicted that the relaxation increases linearly with the thickness as the inclined dislocations thread through the epilayer, which may ultimately lead to a tensile stress at the top of the epilayer.^{12,14} On the other hand, the reduction of TD density and the free volume related to TDs may induce tensile stress in a manner similar to the induction of tensile stress by grain growth and grain boundary annihilation.¹⁵ This also offsets the composition grading-induced compressive stress.⁷

Figure 6b also shows that a compressive-to-tensile stress transition is not apparent for the 500-nm GaN films grown on the single graded $\text{Al}_x\text{Ga}_{1-x}\text{N}$

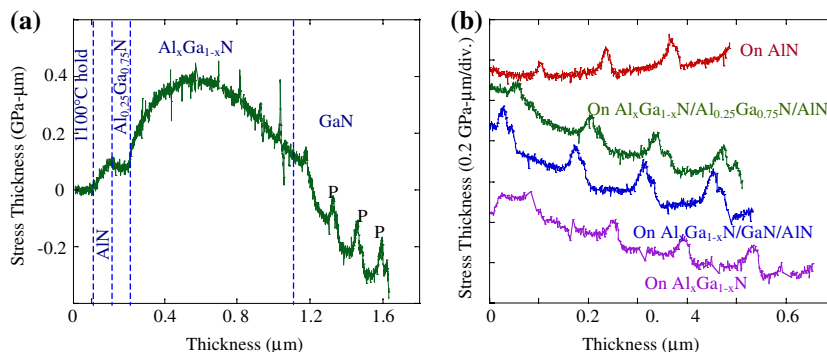


Fig. 6. Stress-thickness product versus thickness of (a) the GaN/ $\text{Al}_x\text{Ga}_{1-x}\text{N}$ / $\text{Al}_{0.25}\text{Ga}_{0.75}\text{N}$ /AlN/Si heterostructure and (b) the GaN films grown on different buffer layers. The dashed lines in (a) separate the different layers.

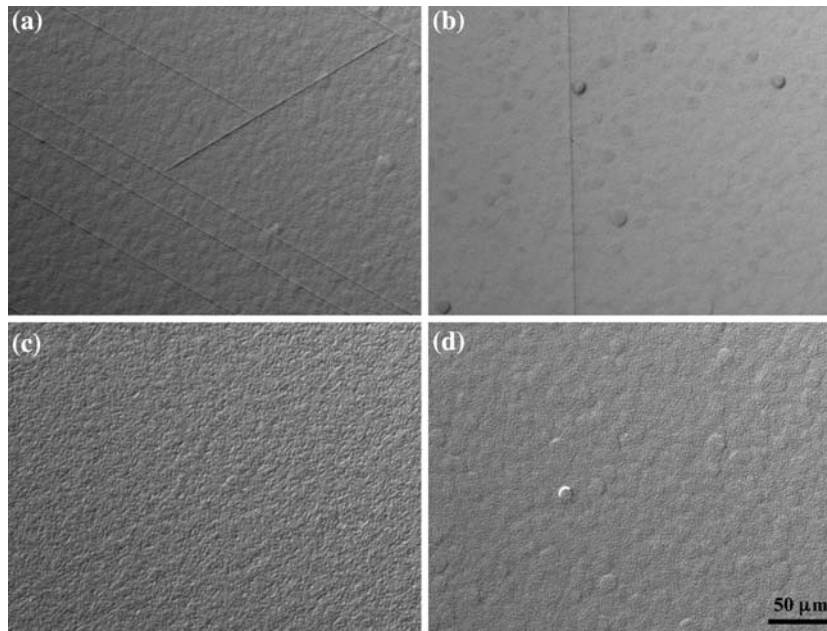


Fig. 7. Optical microscope images of the GaN films grown on (a) a thin AlN buffer layer, (b) a single grade AlGa_{1-x}N buffer layer, (c) an AlN/GaN/Al_xGa_{1-x}N multilayer buffer, and (d) an AlN/Al_{0.25}Ga_{0.75}N/Al_xGa_{1-x}N multilayer buffer. Each image was collected near the center region of a 1 × 1 cm sample.

buffer layer and the multilayer buffers. Thus, the compressive-to-tensile stress transition is significantly delayed for these three films compared to the GaN film grown on the thin AlN buffer layer. This delay correlates with a reduced crack density in these three GaN films. As shown in Fig. 7a, the GaN film on the thin AlN buffer layer is heavily cracked. However, the crack density in films grown on the single graded Al_xGa_{1-x}N buffer layer and the multilayer buffers are significantly reduced, as shown in Fig. 7b–d. Indeed, no cracks near the center of the 1 × 1 cm sample were observed for the GaN film grown on the AlN/Al_{0.25}Ga_{0.75}N/Al_xGa_{1-x}N multilayer buffer. Although cracks are still observed near the edge of each sample, the overall crack density is reduced by using graded Al_xGa_{1-x}N or multilayer buffers instead of a thin AlN buffer layer.

CONCLUSIONS

The evolution of TDs, stress, and cracking of GaN films grown on (111) Si substrates using four different buffer layers has been studied. Compared to that grown on a thin AlN buffer layer, the GaN film grown on a compositionally graded Al_xGa_{1-x}N (0 ≤ x ≤ 1) buffer layer shows significantly reduced TD density. Despite the high initial TD density, the composition grading-induced compressive stress enhances the TD bending and annihilation in the top half of the Al_xGa_{1-x}N layer, which subsequently leads to the TD density reduction in the overgrown GaN film. Furthermore, by growing on an AlN/Al_yGa_{1-y}N/ (y = 0 or 0.25) bilayer instead of growing

directly on the Si substrate, the initial TD density in the Al_xGa_{1-x}N layer can be considerably reduced and the TD density of the overgrown GaN film can be further reduced. The application of the graded Al_xGa_{1-x}N and AlN/Al_yGa_{1-y}N/Al_xGa_{1-x}N (0 ≤ x ≤ 1, y = 0, and 0.25) multilayer buffers also defers the compressive-to-tensile stress transition in the GaN films, which alleviates the cracking of the films.

ACKNOWLEDGEMENTS

This work was supported by The Penn State Electro-Optics Center, the Lehigh-Penn State Center for Optical Technologies, and the National Science Foundation under Grant Nos. ECS-0093742 and DMR-0606451.

REFERENCES

1. A. Watanabe, T. Takeuchi, K. Hirotsawa, H. Amano, K. Hiramatsu, and I. Akasaki, *J. Cryst. Growth* 128, 391 (1993).
2. D.M. Follstaedt, J. Han, P. Provencio, and J.G. Fleming, *MRS Internet J. Nitride Semicond. Res.* 4S1, G3.72 (1999).
3. S. Raghavan and J.M. Redwing, *J. Appl. Phys.* 98, 023514 (2005).
4. H. Marchand, L. Zhao, N. Zhang, B. Moran, R. Coffie, U.K. Mishra, J.S. Speck, S.P. DenBaars, and J.A. Freitas, *J. Appl. Phys.* 89, 7846 (2001).
5. A. Able, W. Wegscheider, K. Engl, and J. Zweck, *J. Cryst. Growth* 276, 415 (2005).
6. S. Raghavan and J.M. Redwing, *J. Appl. Phys.* 98, 023515 (2005).
7. S. Raghavan, X. Weng, E.C. Dickey, and J.M. Redwing, *Appl. Phys. Lett.* 88, 041904 (2006).
8. X. Weng, S. Raghavan, E.C. Dickey, and J.M. Redwing, *Mater. Res. Soc. Symp. Proc.* 892, 0892-FF02-02.1 (2006).

9. X. Weng, S. Raghavan, J.D. Acord, A. Jain, E.C. Dickey, and J.M. Redwing, *J. Cryst. Growth* (in press).
10. G.G. Stoney, *Proc. R. Soc. London, Ser. A*82, 172 (1909).
11. S. Raghavan and J.M. Redwing, *J. Cryst. Growth* 261, 294 (2004).
12. D.M. Follstaedt, S.R. Lee, P.P. Provencio, A.A. Allerman, J.A. Floro, and M.H. Crawford, *Appl. Phys. Lett.* 87, 121112 (2005).
13. P. Cantu, F. Wu, P. Waltereit, S. Keller, A.E. Romanov, U.K. Mishra, S.P. DenBaars, and J.S. Speck, *Appl. Phys. Lett.* 83, 674 (2003).
14. A.E. Romanov and J.S. Speck, *Appl. Phys. Lett.* 83, 2569 (2003).
15. P. Chaudhari, *J. Vac. Sci. Technol.* 9, 520 (1972).